



HAL
open science

Low-temperature aging of Y-TZP ceramics

Jérôme Chevalier, Bernard Cales, Jean Michel Drouin

► **To cite this version:**

Jérôme Chevalier, Bernard Cales, Jean Michel Drouin. Low-temperature aging of Y-TZP ceramics. *Journal of the American Ceramic Society*, 1999, 82 (8), pp.2150-2154. 10.1111/j.1151-2916.1999.tb02055.x . hal-01677824

HAL Id: hal-01677824

<https://hal.science/hal-01677824>

Submitted on 6 Apr 2023

HAL is a multi-disciplinary open access archive for the deposit and dissemination of scientific research documents, whether they are published or not. The documents may come from teaching and research institutions in France or abroad, or from public or private research centers.

L'archive ouverte pluridisciplinaire **HAL**, est destinée au dépôt et à la diffusion de documents scientifiques de niveau recherche, publiés ou non, émanant des établissements d'enseignement et de recherche français ou étrangers, des laboratoires publics ou privés.



Distributed under a Creative Commons Attribution 4.0 International License

Low-Temperature Aging of Y-TZP Ceramics

Jérôme Chevalier

National Institute of Applied Sciences, Department of Research into the Metallurgy and Physical Properties of Materials, Associate Research Unit 5510, 69621 Villeurbanne Cedex, France

Bernard Cales* and Jean Michel Drouin

Norton Desmarquest Fine Ceramics, 27025 Evreux Cedex, France

The isothermal tetragonal-to-monoclinic transformation of a 3Y-TZP ceramic is investigated from 70° to 130°C in water and in steam by X-ray diffraction and optical interferometer techniques. Aging kinetics followed by X-ray diffraction are fitted by the Mehl–Avrami–Johnson law, suggesting nucleation and growth to be the key mechanisms for transformation. Optical interferometer observations of highly polished samples effectively reveal a nucleation and growth micromechanism for tetragonal-to-monoclinic transformation. A model based on surface change analysis is developed that fits closely to the X-ray diffraction results.

I. Introduction

THE concept of stress-induced phase transformation in zirconia ceramics represents one of the most remarkable innovations in the ceramic field. Indeed, it was shown in the 1970s, first by Garvie *et al.*¹ and then by Gupta *et al.*,² that zirconia exhibits a transformation toughening mechanism acting to resist crack propagation. The stress-induced phase transformation involves the transformation of metastable tetragonal crystallites to the monoclinic phase at the crack tip, which, accompanied by a volumetric expansion, induces compressive stresses. Yttria-stabilized zirconia ceramics belong to this family of toughened materials. They can exhibit a strength of more than 1000 MPa with a toughness of about 6 to 10 MPa · m^{1/2}. Experimental^{3–5} and theoretical^{6,7} studies agree that transformation toughening is highly dependent on grain size and stabilizer (yttria) content. The excitement created by these materials, however, was dampened by Kobayashi *et al.*,⁸ who discovered a serious limitation of Y-TZP ceramics for applications near 250°C. The authors revealed that Y-TZP ceramics can suffer a slow, tetragonal-to-monoclinic (*t*–*m*) transformation at the sample surface in a humid atmosphere, followed by microcracking and a loss in strength. Following this work, a series of papers were published with an attempt to understand the basic micromechanisms of *t*–*m* transformation and to reduce this limiting phenomenon.^{9–16} The main features of this so-called low-temperature degradation (LTD) are the following:

- (i) Transformation proceeds most rapidly at temperatures of 200–300°C and is time dependent.
- (ii) Water or water vapor enhances the transformation.
- (iii) Transformation proceeds from the surface to the bulk of zirconia materials.
- (iv) Higher stabilizing content or finer grain size increases the resistance to transformation.

Today there are several models which attempt to explain how the presence of water can promote transformation. Sato *et al.*^{10,11} proposed chemisorption of water to form Zr–OH at the surface, which results in the accumulation of strain energy and thus in *t*–*m* transformation. Yoshimura *et al.*¹⁷ also proposed the chemisorption of water as the key mechanism but attributed the accumulation of stresses to the migration of OH[–] species at the surface and in the lattice. A third model, presented by Lange and co-workers,⁹ postulates a reaction between H₂O and yttria (Y₂O₃), the formation of Y(OH)₃ depleting the stabilizer content then leading to transformation. However, recently, the depletion of Y₂O₃ during LTD has been rejected and the fundamental role of internal stresses has been demonstrated.¹⁸

Transformation kinetics have sometimes been fitted by the Mehl–Avrami–Johnson (MAJ) law,^{19,20} which suggests nucleation and growth. However, the evidence for the real nucleation and growth mechanism has never been clearly identified at the surface of Y-TZP materials. This was the aim of the present study, to identify nucleation and growth processes occurring during LTD. Another question is the extent of isothermal transformation at low temperature, typically near room temperature. Therefore, an attempt was made to provide LTD data at low temperatures, far below 150°C, in order to predict accurately isothermal *t*–*m* transformation kinetics of zirconia ceramics for low-temperature applications.

II. Experimental Procedure

The experiments were conducted on a Y-TZP ceramic containing 3 mol% (5.2 wt%) yttria (Norton Desmarquest Fine Ceramics, France). The commercial starting powder was produced by a coprecipitation method. The material was processed by cold isostatic pressing at 300 MPa, followed by pressureless sintering at 1500°C for 2 h. Hot isostatic pressing was then conducted to achieve a density of more than 99.9%. The grain size was measured by SEM according to the ASTM E112 standard. The average grain size value by linear intercept was 0.5 μm. Small disks of 40 mm diameter and 4 mm thickness were ground and polished with diamond paste to reach a surface roughness (R_a) of less than 3 nm (measured by means of an optical interferometer, Phase Shift Technology®). Such a roughness was believed to be low enough to observe any small surface uplift due to *t*–*m* transformation. No annealing was done on the specimens because it was shown that monoclinic content and residual grinding stresses were suppressed during careful polishing steps.²¹ Monoclinic content was measured by an X-ray diffraction (XRD) technique (CuK α radiation, with a penetration depth in zirconia estimated to be about 5 μm from Ref. 22) and calculated from the modified Garvie and Nicholson equation.²³ It was systematically close to 0% before any aging test. Surface changes were recorded by means of the optical interferometer used for roughness measurements in a

*Member, American Ceramic Society.

monochromatic wavelength mode. It is characterized by a height resolution of ± 0.1 nm (X - Y resolution of about $0.3 \mu\text{m}$). Aging was achieved in distilled water at different temperatures from 70° to 100°C (thermostated baths $\pm 2^\circ\text{C}$) and in steam at 120°C and 130°C under 2 bar.

III. X-ray Diffraction Results

The relationship between the amount of monoclinic phase and aging time at various temperatures is shown in Fig. 1. The amount of monoclinic phase increases with aging time according to a sigmoidal behavior, in agreement with previous studies conducted at high temperatures.^{24–26} These studies suggested that the relationship between the amount of monoclinic phase and the aging time could be expressed by the MAJ equation:^{19,20}

$$f = 1 - \exp[-(b \cdot t)^n] \quad (1)$$

where f is the transformation fraction, t is the time, and b and n are constants. The MAJ equation is often used for describing time-transformation isotherms in metals and metallic alloys. Tsubakino *et al.*^{24,25} suggested that isothermal transformation occurs by a nucleation and growth process without providing experimental evidence for this mechanism. In the MAJ theory summarized by Christian,²⁰ it is shown that the n exponent, which can be derived from the slope of the $\ln(\ln(1/(1-f)))$ versus $\ln t$ plot, is related to nucleation and growth conditions. b is a parameter giving the apparent activation energy Q by

$$b = b_0 \exp\left[-\frac{Q}{RT}\right] \quad (2)$$

where b_0 is a constant, R the gas constant and T the absolute temperature. b can also be calculated for each temperature from a $\ln(\ln(1/(1-f)))$ versus $\ln t$ plot. This plot is shown in Fig. 2. Because the monoclinic fraction never reaches 100% even after a very long duration, f is taken as the fraction in the saturated amount of monoclinic phase (88%). A linear relationship is observed for each temperature with a constant value of n equal to 3.6 ± 0.4 . According to the MAJ theory,^{19,20} this value between 3 and 4 corresponds to a nucleation and three-dimensional growth process. The plot of $\ln b$ versus $1/T$ in Fig. 3 gives an activation energy of 106 kJ/mol with excellent reliability (correlation coefficient of more than 99%).

IV. Optical Interferometer Investigations

The nucleation and growth mechanism for LTD, which was suggested by XRD, was confirmed by optical interferometer

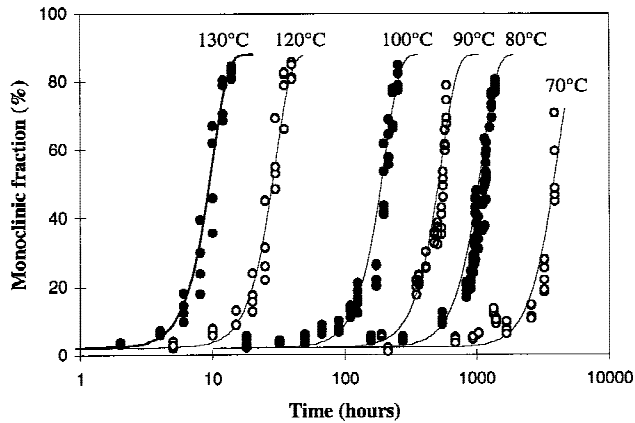


Fig. 1. Monoclinic content measured by X-ray diffraction versus time for temperatures ranging from 70° to 130°C . Solid lines represent the fitting of the experimental results by the Mehl-Avrami-Johnson law with $n = 3.6$.

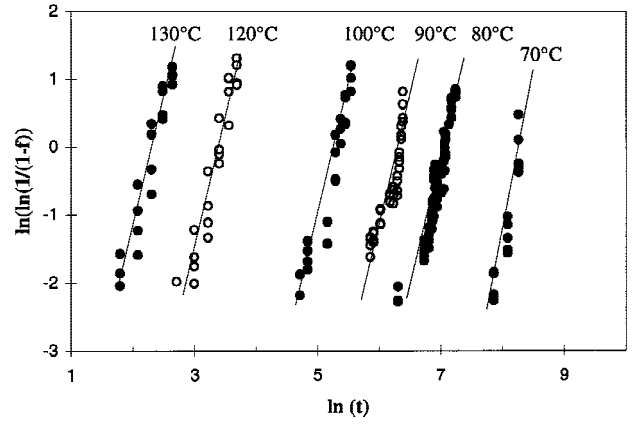


Fig. 2. Plot of $\ln(\ln(1/(1-f)))$ versus $\ln t$ for the determination of n (slope) and $\ln b$ (ordinate origin) in the MAJ equation.

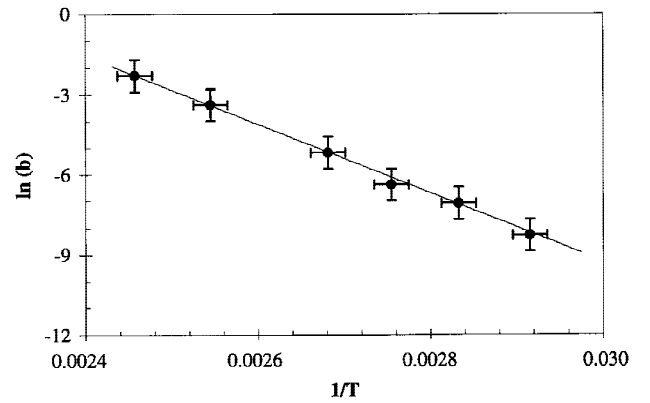


Fig. 3. Plot of $\ln b$ versus $1/T$ for the determination of the apparent activation energy for the t - m phase transformation process.

observations. For instance, Fig. 4 represents the same surface of a given specimen observed with the optical interferometer after different aging durations at 130°C , 2 bar in steam. Figure 4(a) corresponds to the initial surface, with a roughness $R_a = 2$ nm and a monoclinic content close to 0%. After an incubation period of about 1 h, the nucleation of monoclinic sites occurs (see Fig. 4(b)). Nucleation is detected by small surface upheavals (with a height less than 10 nm and a diameter close to $1 \mu\text{m}$) which correspond to the transformation of one or a few grains.^{27,28} This surface expansion is linked to the increase of the crystal size and thus the grain size due to t - m transformation. At that time, monoclinic fraction measured with XRD still remains close to 0%. After 5 h (in Fig. 4(c)), it appears that the initial nucleation sites have slightly increased in size. Their shape is nearly conical, suggesting that transformation effectively occurs from one grain to the neighboring grains and so on. The propagation from the initially transformed grain to the others is related to the formation of micro- or nanocracks around transformed grains, as already suggested by several authors. In addition to the initial sites, new nucleation sites are created (Fig. 4(c)). Monoclinic content measured by XRD now reaches 10%. It is observed that the “conical” monoclinic sites grow at an approximately constant rate with time, with a constant ratio of height/diameter of about 1%. Figure 4(d) shows the same surface after 7 h for a monoclinic fraction of 20% and confirms a nucleation and growth process.

Saturation in monoclinic content measured by XRD is reached at the time when the surface is completely covered by conical spots. Transformation then proceeds in the bulk of the material (i.e., deeper than the first $5 \mu\text{m}$ analyzed by X-ray diffraction analysis).

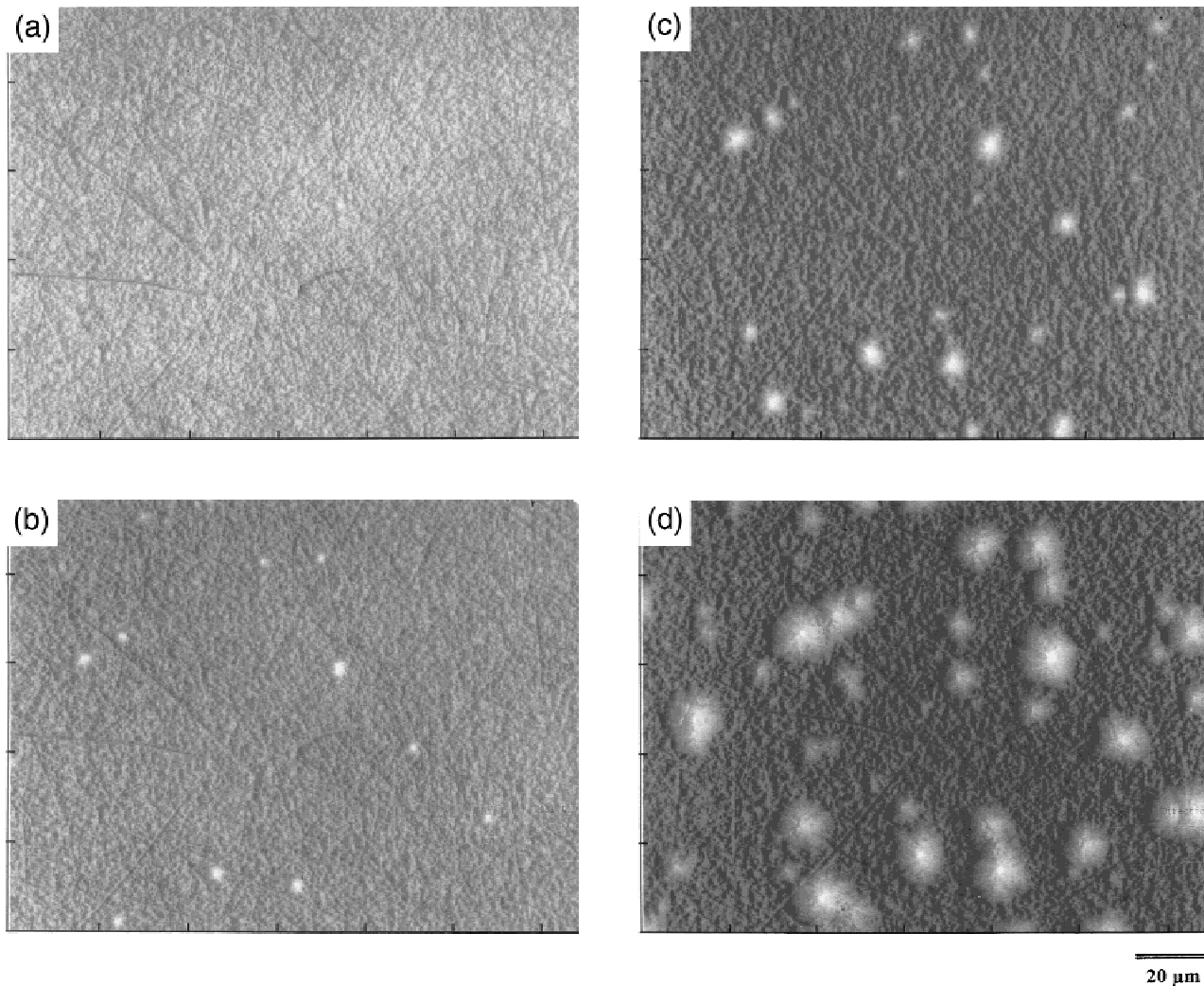


Fig. 4. Optical interferometer observation of the same area ($165 \times 124 \mu\text{m}^2$): (a) before aging for a monoclinic fraction f close to 0%, (b) after 3 h in steam at 134°C , 2 bar with $f < 5\%$, (c) 5 h with $f = 10\%$, and (d) 7 h with $f = 20\%$.

V. Analysis and Discussion

Figure 5(a) shows the diameter and the height of three particular conical surface upheavals as a function of time after their nucleation, at 130°C . The plots can be fitted with linear

relationships. The nucleation rate at 130°C is followed in Fig. 5(b) for two regions of the same specimen (area of each region: $165 \times 124 \mu\text{m}^2$) from the beginning of the LTD until the surface is totally recovered by monoclinic grains. After a short apparent incubation period of about 1 h, the number of nuclei

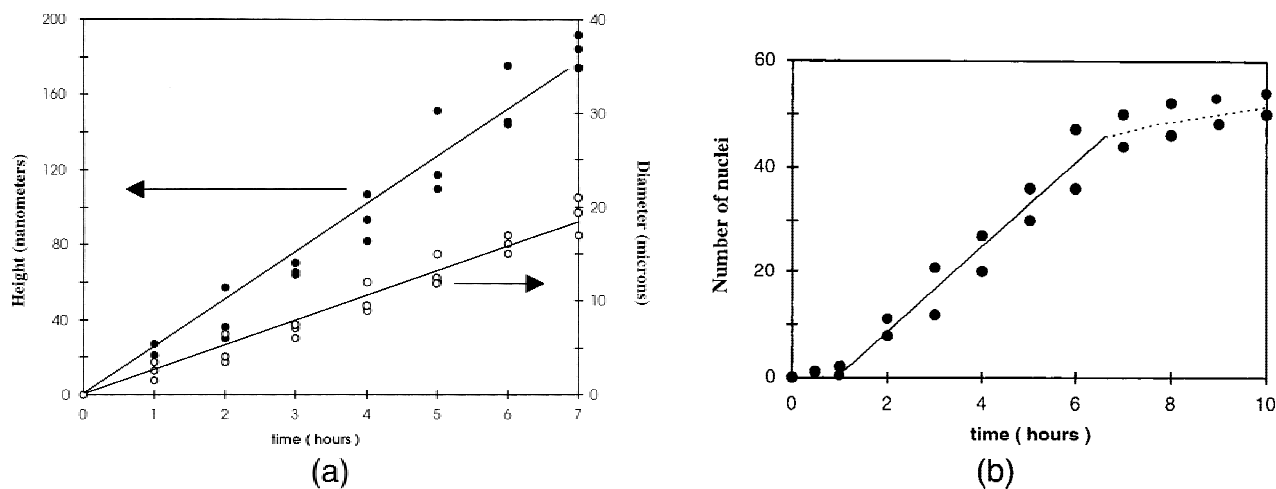


Fig. 5. Variation of spot size (height and diameter) (a) and nuclei number (b) with time for the evaluation of the α_c , α_h , and N_r parameters.

varies linearly with time, the nucleation rate being constant. After 7 h, i.e., for a monoclinic content higher than 30%, the nucleation rate reaches a saturation level. Such a saturation level can result from compressive stresses induced by the t - m transformation.²¹ Another explanation for the saturation is the decrease of the probability of nucleation at a given location as LTD proceeds at sites distributed randomly. The optical analysis can therefore be summarized in a mathematical form, for monoclinic content less than 30%:

$$d_r(t) = \alpha_d(t - \tau) \quad (3)$$

$$h_r(t) = \alpha_h(t - \tau) \quad (4)$$

$$dN = N_r A d\tau \quad (5a)$$

where $d_r(t)$ and $h_r(t)$ represent the diameter and the height of a spot originating at time $t = \tau$, and where dN corresponds to the number of nuclei created between τ and $\tau + d\tau$, α_d and α_h are constants characteristic of the diameter and height growth rates, and N_r is the nucleation rate per unit time and area. A is the area observed for the analysis. The surface uplift observed at the surface corresponds to the volume expansion due to t - m transformation, known to be accompanied by a volume expansion of about 4%,²⁹ thus by a linear expansion, k , of about 1.3%. Thus, the volume of a given monoclinic region originating at $t = \tau$ is given by

$$v_r(t) = \frac{\pi}{12} \frac{\alpha_d^2 \alpha_h}{k} (t - \tau)^3 \quad (6)$$

During the initial period of LTD, when nuclei are widely spaced and the interaction between them is negligible, the monoclinic volume at time t resulting from nuclei created between τ and $\tau + d\tau$ is $dV_m = v_r(t) dN$. Thus, the total transformed volume at time t is equal to

$$V_m = \int_0^t \frac{\pi}{12} \frac{\alpha_d^2 \alpha_h}{k} N_r A (t - \tau)^3 d\tau \quad (7)$$

The integration of Eq. (7) gives

$$V_m = N_r \frac{\pi}{48} \frac{\alpha_d^2 \alpha_h}{k} A t^4 \quad (8)$$

The following constants can be derived from Figs. 5(a) and (b): $\alpha_d = 2.7 \mu\text{m/h}$, $\alpha_h = 27 \times 10^{-3} \mu\text{m/h}$, and $N_r = 3.7 \times 10^{-4} \text{h}/\mu\text{m}^2$. The monoclinic fraction, f , calculated for a layer of material of thickness, l , is equal to

$$f = \frac{V_m}{Al} = \frac{N_r}{l} \frac{\pi}{48} \frac{\alpha_d^2 \alpha_h}{k} t^4 \quad (9a)$$

Therefore, with $k = 1.3\%$, and with $l = 5 \mu\text{m}$ (to compare with the monoclinic fraction obtained with the XRD analysis), the monoclinic fraction at 130°C is

$$f_{(\%) } = 0.0072t^4 \quad (9b)$$

The monoclinic fraction calculated at 130°C using Eq. (9a) is plotted in Fig. 6 and compared with the experimental X-ray diffraction results. The correlation between the two curves is excellent when the monoclinic content does not exceed 30%. Above 30%, the decrease in nucleation rate is not considered in the analysis. For a more correct analysis we have to consider also the decrease in the tetragonal content, thus the decrease in the probability of nucleation at a given location, with time. A simple refinement then replaces Eq. (5a) by

$$dN = N_r A (1 - f) d\tau \quad (5b)$$

The combination of Eqs. (5b) and (6) gives

$$\frac{df}{1-f} = \frac{\pi \alpha_d^2 \alpha_h N_r}{12kl} (t - \tau)^3 d\tau \quad (10)$$

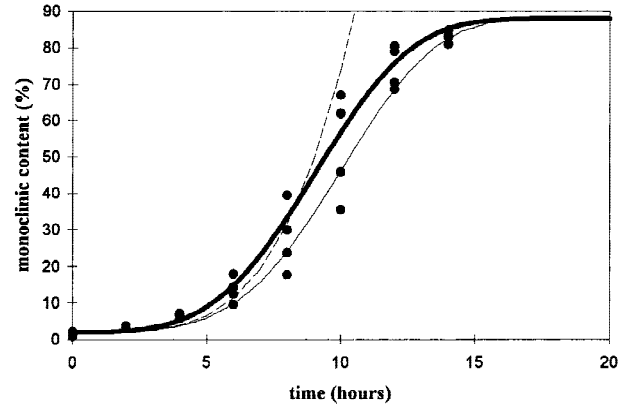


Fig. 6. Variation of monoclinic content with time at 130°C, 2 bar in steam from X-ray diffraction results (●), MAJ equation with $n = 3.6$ (heavy line), Eq. (9a) (dotted line), and Eq. (11) (single line) of the nucleation and growth model.

The monoclinic fraction is then obtained by integration of Eq. (10):

$$f = 1 - \exp \left[- \left(\frac{\pi \alpha_d^2 \alpha_h N_r}{48kl} \right) t^4 \right] \quad (11)$$

The monoclinic fraction f calculated from Eq. (11) is also plotted in Fig. 6 and compared to XRD results. The agreement is very good. Also remarkable is the similarity between Eq. (11) from the present analysis and Eqs. (1) and (2) from the MAJ treatment, with $b = [\pi \alpha_d^2 \alpha_h N_r / 48kl]^{1/n}$. The present analysis leads to a value of 4 for the n exponent, while experimental X-ray diffraction results lead to a value of about 3.6. The slight difference can result from the compressive stresses induced by t - m transformation and which hinder the nucleation and, maybe, the growth rate. These compressive stresses are not considered in the present analysis.

It is of prime interest then to determine the temperature dependence of the constants α_d , α_h , and N_r . This was done by recording the nucleation rate and the nuclei growth rates at four temperatures: 80°, 100°, 120°, and 130°C. The variation of α_d , α_h , and N_r versus temperature is recorded in Fig. 7 in Arrhenius plots to derive the activation energy. It is not surprising to obtain three, parallel, straight lines, giving each an activation energy of about 100 kJ/mol, similar to that calculated from XRD results by the MAJ equation.

VI. Conclusion

The low-temperature degradation behavior of a 3Y-TZP ceramic was investigated from 70° to 130°C. X-ray diffraction

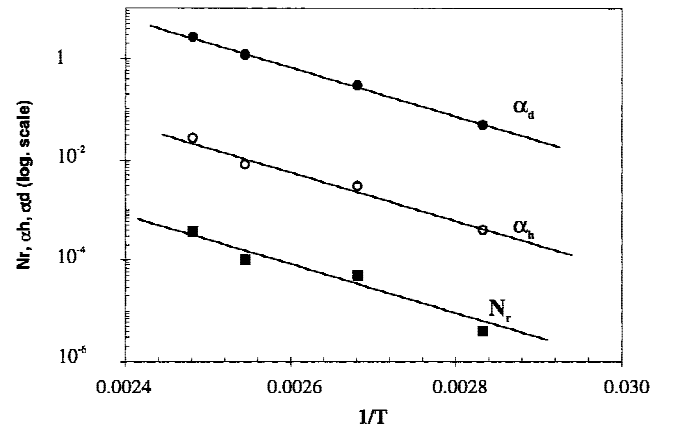


Fig. 7. Variation of α_d , α_h , and N_r with temperature.

results suggested an incubation–nucleation–growth mechanism for transformation because of sigmoidal variation of the monoclinic fraction with time for all temperatures. The MAJ equation was used to fit the experimental data, with $n = 3.6$. Nucleation and growth micromechanisms were then confirmed with optical interferometer observations on highly polished surfaces. A model was used that correlated well with the MAJ law. This equation allows an accurate prediction of the monoclinic fraction at the surface of the aged 3Y-TZP ceramic for a given time and temperature and particularly for low-temperature applications.

This study was focused on a given zirconia ceramic. Any extrapolation to other zirconia ceramics could be subjected to large error because LTD is primarily dependent on the ceramic microstructure (grain, size, yttrium content, density, etc.). Therefore, LTD parameters should be specifically determined for each Y-TZP ceramic.

Acknowledgments: We would like to thank O. Filippini for his help with the experimental work and Ed Leivadnik for helpful comments on the manuscript.

References

- ¹R. C. Garvie, R. H. J. Hannink, and R. T. Pascoe, "Ceramic Steel?" *Nature (London)*, **258**, 703–4 (1975).
- ²T. K. Gupta, F. F. Lange, and J. H. Bechtold, "Effect of Stress-Induced Phase Transformation on the Properties of Polycrystalline Zirconia-Containing Tetragonal Phase," *J. Mater. Sci.*, **13**, 1464–70 (1978).
- ³F. Lange, "Transformation Toughening, Part III, Experimental Observations in the ZrO_2 - Y_2O_3 System," *J. Mater. Sci.*, **17**, 240–46 (1982).
- ⁴M. V. Swain, "Grain Size Dependence of Toughness and Transformability of 2 mol% Y-TZP Ceramics," *J. Mater. Sci. Lett.*, **5**, 1159–61 (1986).
- ⁵V. Gross and M. V. Swain, "Mechanical Properties and Microstructure of Sintered and Hot Isostatically Pressed Ytria-Partially Stabilized Zirconia," *J. Aust. Ceram. Soc.*, **22**, 1–7 (1986).
- ⁶F. F. Lange, "Transformation Toughening, Part I and Part II," *J. Mater. Sci.*, **17**, 225–40 (1982).
- ⁷D. J. Green, R. H. J. Hannink, and M. V. Swain, *Transformation Toughening of Ceramics*. CRC Press, Boca Raton, FL, 1989.
- ⁸K. Kobayashi, H. Kuwajima, and T. Masaki, "Phase Change and Mechanical Properties of ZrO_2 - Y_2O_3 Solid Electrolyte After Ageing," *Solid State Ionics*, **3/4**, 489–95 (1981).
- ⁹F. F. Lange, G. L. Dunlop, and B. I. Davis, "Degradation During Ageing of Transformation-Toughened ZrO_2 - Y_2O_3 Materials at 250°C," *J. Am. Ceram. Soc.*, **69**, 237–40 (1986).
- ¹⁰T. Sato and M. Shimada, "Transformation of Ytria-Doped Tetragonal ZrO_2 Polycrystal by Annealing in Water," *J. Am. Ceram. Soc.*, **68**, 356–59 (1985).
- ¹¹T. Sato, S. Ohtaki, and T. Endo, "Transformation of Ytria Doped Tetrag-

onal Zirconia Polycrystals by Annealing under Controlled Humidity Conditions," *J. Am. Ceram. Soc.*, **68**, C-230 (1985).

¹²K. Nakajima, K. Kobayashi, and Y. Murata, "Phase Stability of Y-PSZ in Aqueous Solutions"; pp. 399–407 in *Advances in Ceramics*, Vol. 12, *Science and Technology of Zirconia*. Edited by N. Claussen, M. Rühle, and A. H. Heuer. American Ceramic Society, Columbus, OH, 1984.

¹³K. Tsukuma, Y. Kubota, and T. Tsukidate, "Thermal and Mechanical Properties of Y_2O_3 Stabilized Zirconia Polycrystals"; pp. 382–90 in *Advances in Ceramics*, Vol. 12, *Science and Technology of Zirconia*. Edited by N. Claussen, M. Rühle, and A. H. Heuer. American Ceramic Society, Columbus, OH, 1984.

¹⁴M. Watanabe, S. Iios, and L. Fukuura, "Aging Behavior of Y-TZP"; pp. 391–98 in *Advances in Ceramics*, Vol. 12, *Science and Technology of Zirconia*. Edited by N. Claussen, M. Rühle, and A. H. Heuer. American Ceramic Society, Columbus, OH, 1984.

¹⁵J. Feng-Li and R. Watanabe, "Influence of a Small Amount of Al_2O_3 Addition on the Transformation of Y_2O_3 Partially Stabilized ZrO_2 during Annealing," *J. Mater. Sci.*, **32**, 1149–53 (1997).

¹⁶M. Hirano, "Inhibition of Low Temperature Degradation of Tetragonal Zirconia Ceramics—A Review," *Br. Ceram. Trans. J.*, **91**, 139–47 (1992).

¹⁷M. Yoshimura, T. Noma, K. Kawabata, and S. Somiya, "Role of Water on the Degradation Process of Y-TZP," *J. Mater. Sci. Lett.*, **6**, 465–67 (1987).

¹⁸D. J. Kim, H. J. Jung, and D. H. Cho, "Phase Transformation of Y_2O_3 and Nb_2O_5 Doped Tetragonal Zirconia during Low Temperature Ageing in Air," *Solid State Ionics*, **80**, 67–73 (1995).

¹⁹W. A. Johnson and R. F. Mehl, "Reaction Kinetics in Processes of Nucleation and Growth," *Trans. Am. Inst. Min., Metall. Pet. Eng.*, **135**, 416–41 (1939).

²⁰J. W. Christian, *The Theory of Transformations in Metals and Alloys*, 2nd ed.; pp 1–19. Pergamon Press, Oxford, U.K., 1965.

²¹J. Chevalier, "Slow Crack Growth Behavior of 3Y-TZP Biomedical Ceramics" (in Fr.); Ph.D. Thesis. National Institute of Applied Sciences of Lyon, Lyon, France, 1996.

²²J. Emsley, *The Elements*, 2nd ed. Oxford University Press, Oxford, U.K., 1991.

²³R. C. Garvie and P. S. Nicholson, "Phase Analysis in Zirconia Systems," *J. Am. Ceram. Soc.*, **55**, 303–305 (1972).

²⁴H. Tsubakino, M. Hamamoto, and R. Nozato, "Tetragonal-to-Monoclinic Phase Transformation during Thermal Cycling and Isothermal Ageing in Partially Stabilized Zirconia," *J. Mater. Sci.*, **26**, 5521–26 (1991).

²⁵H. Tsubakino, K. Sonoda and R. Nozato, "Martensite Transformation Behavior during Isothermal Ageing in Partially Stabilized Zirconia with or without Alumina Addition," *J. Mater. Sci.*, **12**, 196–98 (1993).

²⁶W. Zhu, T. Lei, and Y. Zhou, "Time-Dependent Tetragonal-to-Monoclinic Transition in Hot-Pressed Zirconia Stabilized with 2 mol% Ytria," *Mater. Chem. Phys.*, **34**, 317–20 (1993).

²⁷C. M. Wayman, "Martensitic Transformation"; pp. 64–81 in *Advances in Ceramics*, Vol. 3, *Science and Technology of Zirconia*. Edited by A. H. Heuer and L. W. Hobbs. American Ceramic Society, Columbus, OH, 1981.

²⁸J. K. Lee and H. Kim, "Surface Crack Initiation in 2Y-TZP Ceramics by Low Temperature Ageing," *Ceram. Int.*, **20**, 413–18 (1994).

²⁹P. M. Kelly and C. J. Ball, "Crystallography of Stress-Induced Martensitic Transformation in Partially Stabilized Zirconia," *J. Am. Ceram. Soc.*, **65**, 242–46 (1986). □